Published in final edited form as:
Cell Metab. 2011 June 8; 13(6): 679–689. doi:10.1016/j.cmet.2011.03.022.

Insulin receptor-related receptor as an extracellular alkali sensor

Igor E. Deyev[1], **Fabien Sohet**[2,3], **Konstantin P. Vassilenko**[4], **Oxana V. Serova**[1], **Nadezhda V. Popova**[1], **Sergey A. Zozulya**[1], **Elena B. Burova**[4], **Pascal Houillier**[2,3,5], **Dmitry I. Rzhevsky**[6], **Anastasiya A. Berchatova**[6], **Arkady N. Murashev**[6], **Anton O. Chugunov**[7], **Roman G. Efremov**[7], **Nikolai N. Nikol'sky**[4], **Eugenio Bertelli**[8], **Dominique Eladari**[2,3,5], and **Alexander G. Petrenko**[1,*]

[1]Laboratory of Receptor Cell Biology, Shemyakin-Ovchinnikov Institute of Bioorganic Chemistry, Russian Academy of Sciences, Moscow 117997, Russia

[2]Université Paris Descartes; INSERM UMRS 872, Equipe 3; centre de Recherche des cordeliers, 15 rue de l'Ecole de Médecine, F-75006, Paris, France

[3]Université Pierre et Marie Curie; and CNRS ERL7226, 15 rue de l'Ecole de Médecine, F-75006, Paris, France

[4]Department of Intracellular Signaling and Transport, Institute of Cytology, Russian Academy of Sciences, St Petersburg 194064, Russia

[5]Hopital Européen Georges Pompidou, Département de Physiologie, Assistance Publique-Hopitaux de Paris, 20 rue Leblanc, F-75015, Paris, France

[6]Biological Testing Laboratory, Branch of Shemyakin-Ovchinnikov Institute of Bioorganic Chemistry, Russian Academy of Sciences, Pushchino 142290, Russia

[7]Laboratory of Biomolecular Modeling, Shemyakin-Ovchinnikov Institute of Bioorganic Chemistry, Russian Academy of Sciences, Moscow 117997, Russia

[8]Department of Physiopathology, Experimental Medicine and Public Health, University of Siena, 53100 Siena, Italy

SUMMARY

The insulin receptor-related receptor (IRR), an orphan receptor tyrosine kinase of the insulin receptor family, can be activated by alkaline media both *in vitro* and *in vivo* at pH>7.9. The alkali-sensing property of IRR is conserved in frog, mouse and human. IRR activation is specific, dose-dependent, quickly reversible and demonstrates positive cooperativity. It also triggers receptor conformational changes and elicits intracellular signaling. The pH sensitivity of IRR is primarily defined by its L1F extracellular domains. IRR is predominantly expressed in organs that come in contact with mildly alkaline media. In particular, IRR is expressed in the cell subsets of the kidney that secrete bicarbonate into urine. Disruption of IRR in mice impairs the renal response to alkali loading attested by development of metabolic alkalosis and decreased urinary bicarbonate excretion in response to this challenge. We therefore postulate that IRR is an alkali sensor that functions in the kidney to manage metabolic bicarbonate excess.

*To whom correspondence should be addressed. petrenkoag@mail.ru, petrenkoag@gmail.com.

INTRODUCTION

Insulin receptor-related receptor (IRR) is a member of the family of three structurally related receptor tyrosine kinases that includes insulin receptor (IR) and insulin-like growth factor receptor (IGF-IR) (Shier and Watt, 1989; Ullrich et al., 1985; Ullrich et al., 1986). Natural agonists of the latter two are insulin and two insulin-like growth factors, IGF-I and IGF-II. While stimulation of IR with insulin primarily modulates cellular metabolism, the main function of activated IGF-IR is to promote cell proliferation and survival (De Meyts, 2002; Dupont and LeRoith, 2001). Although insulin binds to IR with approximately 100-fold higher binding affinity as compared to IGF-IR, it can also stimulate the latter at higher concentrations; the same is true for IGF-I and IR. In contrast, none of the known IR or IGF-IR ligands can activate IRR (Jui et al., 1994; Zhang and Roth, 1992), and the physiological role of IRR has remained enigmatic primarily because no endogenous ligands for IRR have been identified since its discovery in 1989, despite significant efforts that included the genome analysis (Dissen et al., 2005).

Contrary to the widespread distribution of IR and IGF-IR in different tissues and cell types, IRR is primarily expressed in the kidneys, stomach, and pancreas (Hirayama et al., 1999; Mathi et al., 1995) - organs that exhibit acid or base-transporting epithelia. Chimeric receptors with IRR intracellular signaling domain, fused to other activatable receptors' ectodomains, can signal via insulin-similar pathways that involve insulin receptor substrate-1 (IRS-1) and IRS-2 (Hirayama et al., 1999), as well as GAP-associated p60 and Shc, and results in the stimulation of glucose uptake (Dandekar et al., 1998). Also, chimeras of IRR with BDNF receptor can promote neuronal survival and PC12 cells differentiation (Kelly-Spratt et al., 1999; Kelly-Spratt et al., 2002). Yet, the signaling properties of the IRR kinase domain were found to differ significantly from those of IR and IGF-IR (Klammt et al., 2005).

No overt phenotype under normal conditions was detected in mice with targeted inactivation of the IRR gene (Kitamura et al., 2001) while the triple knockout of IRR, IR and IGF-IR revealed a redundant role of all three receptors in male gonads development (Nef et al., 2003) that has not received any mechanistic explanation. The phylogenetic analysis of the IRR orthologous sequences indicated that IRR, as a separate entity from IR and IGF-IR, evolved in amphibians and remained conserved in mammals. It also revealed a strong selective pressure, suggesting yet unknown important function of IRR (Hernandez-Sanchez et al., 2008; Renteria et al., 2008).

To get an insight into the function of IRR we embarked on a search for endogenous agonist of this receptor. We determined that IRR activation could be achieved by a sole increase in the extracellular pH value. IRR activation by alkaline media was specific, dose-dependent, reversible, determined by the receptor ectodomain and accompanied by a conformational change of the receptor molecule thus resembling typical features of the ligand-receptor interaction. It also triggered the intracellular signaling that involved IRS-1 and AKT/PKB, and involved actin cytoskeleton remodeling. The analysis of $IRR^{-/-}$ mice revealed an impaired renal response to alkali loading attested by decreased urinary bicarbonate excretion, and development of metabolic alkalosis in response to this challenge. Our data suggest a role of IRR as a cell surface alkali-sensing receptor that is involved in renal adaptation to metabolic alkalosis.

RESULTS

IRR activation by alkaline media

Since IRR is primarily found in kidney epithelial cells, we tested several physiological liquids that may come in contact with them, including normal and fetal serum, urine and amniotic fluid, for their ability to stimulate receptor autophosphorylation in cell lines stably transfected with HA-tagged human IRR, and also with IR or IGF-IR as controls. Among several samples analyzed, commercially available amniotic fluid AF-S produced strong and reproducible tyrosine phosphorylation of a protein species corresponding to the size of the phosphorylated IRR β-subunit. In IR-expressing cells, insulin produced strong stimulation, whereas amniotic fluid treatment showed only a minor, if any, effect that could result from endogenous insulin in this fluid (Figure 1A). The stimulatory activity of amniotic fluid was resistant to heat denaturing and was permeable through regular or 1,000 Da cutoff dialysis membranes, but sensitive to mild acidification. Neutralization of the amniotic fluid sample by adjustment to pH 7.4 completely eliminated the IRR response (Figure 1B).

We noted that, among the biological fluids tested, only the AF-S samples of amniotic fluid had pH of about 8.5–9.0, other fluids being neutral or mildly acidic. We therefore tested whether alkaline media, per se, may be the cause of IRR activation. It appeared that a regular cell conditioned medium adjusted to pH 9 produced robust stimulatory effect in IRR-expressing cells whereas neutral media did not produce any response (Figure 1C). Hence, we hypothesized that IRR acts as an alkaline pH sensing receptor.

Preliminary experiments indicated that pH sensitivity of overexpressed IRR was detected in all cell lines tested (Figure 1C, Figure 2A, B and Figure S1A). When the transfected cells were exposed to alkaline media for 50 min, followed by IRR immunoprecipitation and Western blotting with anti-pY antibody, a reliably detectable IRR response was already observed at pH 7.9 (Figure 2B and Figure S1B).

Since IRR evolved in amphibians we tested whether an IRR ortholog from the most distant species also had the alkaline-sensing property. The cDNA of *Xenopus laevis* IRR was expressed as HA-tagged protein in HEK 293 cells and the cells were treated with alkaline media or with insulin. Immunoprecipitation revealed robust activation of the receptor as a result of the treatment with alkali whereas no response to insulin could be detected (Figure 2C).

We also checked whether endogenous IRR in its native environment would retain its pH responsiveness. We treated with alkaline media mouse MIN6 insulinoma cells that were shown to express IRR (Hirayama et al., 1999). The cell lyzates were immunoprecipitated with anti-IRR antibody. Western blotting of the precipitates with antiphosphotyrosine antibody revealed IRR activation only in the sample incubated with the alkaline medium (Figure 2D).

Does IRR activation by alkaline media involve any peptide or protein ligand? Contrary to IR, no basal phosphorylation of IRR was detected in cells, independently of prior starvation, suggesting the absence of endogenous IRR agonists in the serum-containing cell conditioned medium (Figure S1A). We next tested the possibility that the alkali treatment results in secretion of IRR agonist. However, alkaline cell conditioned media, removed from the activated cells after neutralization, did not produce any response in another fresh batch of CHO-IRR cells (Figure S1C). We also performed extensive washing of IRR-transfected cells with large volumes of neutral and alkaline PBS. IRR in the washed cells was still activated by alkaline media, thus ruling out the possibility that any soluble hormone-like substance, resembling insulin or IGF, is involved in the receptor activation (Figure 2E). In a

most simple experiment, we achieved specific IRR activation by simply adding a calculated small amount of sodium hydroxide solution to cells in physiological salt solution as medium (Figure S1D). We also found that IRR remained insensitive to insulin at pH 8.3 (Figure S1E).

IRR activation by a pH change rather than a peptide or protein molecule should be quickly and fully reversible because it does not involve slow-kinetics dissociation of a ligand typically bound by multi-point interactions. To test this assumption, IRR-expressing cells were sequentially treated with alkaline and neutral media. This experiment revealed that, indeed, IRR can be quickly (less than 1 min) dephosphorylated upon neutralization (Figure S1F). When the neutralized cells were further treated with the alkaline medium, IRR was activated again to the same extent (Figure 2E). To determine whether protein tyrosine phosphatases were involved in IRR desensitization, we treated the cells bearing activated IRR with pervanadate prior to neutralization. This treatment abolished IRR dephosphorylation, thus indicating the phosphatase engagement (Figure S1G).

Specificity of IRR activation by alkali

The receptor activation by alkali was specific for IRR as compared to other receptor-like tyrosine kinases. Whereas insulin produced a strong autophosphorylation response in IR and a weaker one in IGF-IR (Figure 3A, central and right sections), but not in IRR (Figure 3A, left section), alkalinization resulted in the activation only of IRR, but not of IR, IGF-IR, or the epidermal growth factor receptor (Figure S2A). Unlike non-specific activation of cellular tyrosine kinases by high-salt buffers, alkali treatment produced a noticeable increase in tyrosine phosphorylation of the IRR but not of other endogenous phosphoproteins (Figure S2B).

It had been shown that insulin binding to IR results in a major conformational change of the receptor. This change could be monitored by the analysis of receptor hydrophobicity in the detergent phase distribution assay (Florke et al., 2001). We analyzed the distribution of HA-tagged IR, IRR and their ectodomain chimera IRR/IR between aqueous and detergent phases induced by warming Triton X-114 extracts of the transfected cells as a function of insulin or alkali addition (Figure 3B and Figure S2C). Insulin binding to IR resulted in a major shift of the ligand-receptor complexes from the detergent (lower) to the aqueous (upper) phase. No change in IRR or IRR/IR distribution was observed upon insulin addition. On the contrary, the adjustment of the extracts pH to 9 induced the transfer of both IRR and IRR/IR to the upper phase without a noticeable effect on the IR distribution. We may therefore conclude that the pH increase induces a conformational change of IRR which is determined by its ectodomain and is essentially similar to the rearrangement of IR that follows the insulin binding.

pH-dependence and positive cooperativity of IRR activation

We observed activation of IRR from pH 7.9 and up to pH 10.5 (Figure S3A), while no activation could be detected by acidic media at pH 5.0 to 7.4 (Figure S3B). To analyze the pH dependence of IRR response in detail, IRR-expressing cells were incubated with a set of Tris-buffered physiological saline solutions with variable pH from 7.4 to 9.2 in small increments. Cell lysates were directly analyzed by Western blotting with anti-phosphoIRR antibody (Figure 4A). For semi-quantitative evaluation, the blots were scanned and the ratio of integral density of the phosphoIRR to the HA bands was plotted versus pH. The resulting plot showed a sigmoid-shaped sharp response with half-effect at pH 8.4 and saturation at about pH 9.0–9.2 (Figure 4B). Interestingly, the activation showed strong positive cooperativity (Hill coefficient 3.5±0.5, calculated by GraphPad Software) in contrast with IR activation by insulin that shows negative cooperativity (De Meyts, 2008). Apparently, the

structural mechanisms of IRR activation are different from the activation of IR that involves the simultaneous interaction of the insulin molecule with two receptor subunits (De Meyts, 2008).

Structural characteristics of IRR activation

To analyze the mechanism of the observed IRR phosphorylation, we prepared two sets of mutants with altered extracellular and intracellular domains of the receptor. As previously reported, mutations of tyrosines 1118 and 1119 at the kinase active site of TrkB/IRR chimera abolished BDNF-induced autophosphorylation and the downstream signaling (Kelly-Spratt et al., 1999). We prepared a similar point mutant of IRR (Figure 5A, left panel). No tyrosine phosphorylation of the mutant was observed upon alkali treatment (Figure 5A, right panel) suggesting that the observed effect was due to autophosphorylation of IRR.

To determine the role of IRR ectodomain in its phosphorylation, we prepared a set of IRR/IR chimeras (Figure 5B, left panel). The first one contained the entire extracellular region of IRR fused with the rest of IR (IRR/IR). The other constructs were made by partial swapping of the extracellular regions of IRR and IR, according to their domain structure. Different combinations of L1, F, and L2 domains of IR were replaced with those of IRR (constructs IRR_L1FL2/IR, IRR_L1F/IR and IRR_L2/IR). The constructs IR_L1FL2/IRR, IR_L1F/IRR and IR_L2/IRR were prepared in an opposite manner by introducing domains of IR into IRR.

The IR/IRR ectodomain chimeras were tested for their response to alkaline media. The replacement of L1FL2 domains in IRR completely abolished receptor sensitivity to alkali. Replacement of either L1F or L2 significantly reduced the receptor response. At the same time, introduction of either L1FL2 or only L1F into IR was sufficient to render alkaline sensitivity (Figure 5B, right panels). In agreement with published work (Kristensen et al., 1999), none of the described chimeras were sensitive to insulin. We may conclude that the key residues that define IRR v.s. IR response are located within L1F domains. Still, other parts of IRR extracellular region are also involved to enhance the response.

To test the correct cell surface expression of these constructs, the transfected HEK 293 cells were biotinylated, lysed and immunoprecipitated with anti-IRR/IR antibody. The Western blots of the precipitates, decorated with streptavidin-HRP and anti-IRR/IR antibody, revealed the appropriate presence of all constructs on the cell surface (Figure S4).

Cellular effects of IRR activation

We further tested whether the IRR activation by alkaline media would produce an intracellular signaling response. It was previously shown that insulin-treated chimera of IR ectodomain, fused with IRR transmembrane and intracellular regions, could be activated with insulin and induced intracellular phosphotyrosine signaling that resulted in insulin-like cell responses (Dandekar et al., 1998; Hirayama et al., 1999). We therefore examined the possibility of whether activation of IRR by alkali can stimulate intracellular signaling pathways similar to those of IR and IGF-IR. The phosphotyrosine staining of IRR-expressing cells, stimulated with alkali, revealed a 170 kDa polypeptide similar by its size to IRS-1, and immunoprecipitation with a specific antibody confirmed the identity of this band as IRS-1 (Figure 6A). In control tests, tyrosine phosphorylation of IRS-1 was observed in cell lines activated by insulin. The pH dependence of IRS-1 activation in CHO-IRR cells was essentially similar to those of IRR with a minor response already detectable at pH 7.8–8.1 (Figure 6B). Our results appear to be in contrast with the reported absence of interaction between IRR and IRS in an *in vitro* binding assay (Klammt et al., 2005). However, they

correlate well with described IRS signaling triggered by IRR chimeras (Hirayama et al., 1999).

We further tested whether other components of the IR/IGF-IR signaling pathway downstream of IRS-1 such as AKT/PKB and ERK1,2 MAP protein kinases can be activated by the alkali treatment of the IRR-expressing cells. AKT phosphorylation (Figure 6C) was detected in IRR-expressing cells. Minor if any AKT phosphorylation was observed in the alkali treated IR-expressing cells that showed a robust response to insulin in a control experiment. Surprisingly, in contrast with insulin treatment, no change of ERK 1,2 basal phosphorylation level in each of three cell lines was detected in response to alkaline stimulation (data not shown).

We also tested if IRR activation would result in any cytoskeleton changes because insulin stimulation was shown to cause actin stress fibers breakdown and appearance of membrane ruffles (Kanzaki, 2006). The IRR, IRR/IR and IR-expressing cells were treated with alkaline media or insulin and stained with phalloidin dye and anti-HA antibody to reveal the receptor presence in particular cell. We noted reorganization of actin fibers and strong blebbing in some IRR-expressing cells as a result of alkali treatment (Figure S5A). A quantitative analysis showed that alkali treatment produced more than a three-fold increase of blebbed cells, bearing IRR. Virtually no such effect was observed in IRR/IR and IR-expressing cells. Interestingly, insulin treatment significantly reduced the number of blebbed cells in CHO-IR and CHO-IRR/IR cell lines (Figure S5B). Thus, the IRR activation can result in cytoskeleton rearrangements, and their specific characteristics are determined by the receptor intracellular domain. While this effect may serve as a whole-cell indicator of IRR activation, it is just an illustration of a cell response and may or may not be related to the physiological role of IRR because of its overexpression in a non-natural system.

Alkali-induced activation of IRR in kidney *in vivo*

We next assessed whether similar phosphorylation of IRR in response to metabolic alkalosis also occurs *in vivo* when IRR is expressed in its natural environment. Since manipulation of extracellular pH in the pancreas or stomach is almost impossible, we chose for this analysis the kidney as the primary organ of IRR expression. Preceding experiments in cell models demonstrated that phosphorylation of IRR is a transient phenomenon (Figure S1F). Thus, to maximize our chances to detect IRR modifications *in vivo*, we designed an experiment in which kidneys of a live anesthetized rat were subjected to acute experimental alkalosis by injecting sodium bicarbonate solution into renal arteries. The kidneys were removed when pH of urine reached mildly alkaline levels of pH ~ 8, typically within 10–15 min. The kidneys were immediately homogenized in a buffer with protease and phosphatase inhibitors, a crude membrane fraction was isolated and further extracted with a mild detergent buffer. The extracts were precipitated with anti-IRR/IR or control antibodies and Western blotted with anti-phosphotyrosine antibody. As control, kidneys, perfused with similar amount of PBS pH 7.4, were used. Blot staining revealed the phosphorylated band of about 66 kDa that indicated autophosphorylation of activated IRR (Figure 7A).

Kidney function deficiency in IRR knockout mice

The physiological relevance of IRR as an alkali sensor was then assessed by testing the effects of IRR disruption in mice subjected to alkali-loading. Wild-type and IRR knockout mice were administered $NaHCO_3$ in their drinking water for 7 days, a treatment that has been shown in mice or rat to induce mild metabolic alkalosis (Sabolic et al., 1997; Wagner et al., 2002), and acid-base parameters, obtained before and after alkali loading, were compared. A control group consisted of mice, receiving NaCl 0.28M instead of $NaHCO_3$, to match the sodium load. Figure 7B shows that $IRR^{+/+}$ mice were able to cope with the alkali

load while *IRR*$^{-/-}$ mice developed compensated metabolic alkalosis. No changes in blood gas parameters were observed following administration of NaCl 0.28M (Figure S6A, S6B).

Alkali loading normally results in increased urine pH and bicarbonate excretion, both of which reaching maximal values within a few hours. Renal bicarbonate excretion depends upon the filtered load of bicarbonate (i.e. plasma [HCO_3^-] x glomerular filtration rate) and also upon renal tubular absorption of bicarbonate. We reasoned that impaired renal excretion of bicarbonate might be detectable only during the initial phase of loading, and not at steady state when *IRR*$^{-/-}$ mice exhibit higher plasma [HCO_3^-] values than controls. We therefore assessed the effects of alkali loading on urine pH and bicarbonate excretion within the first 6 hours and then 24 hours following the beginning of loading. Alkali loading induced a very rapid increase in urine pH and bicarbonate excretion in WT mice. In contrast, the initial response was clearly blunted in *IRR*$^{-/-}$ mice (Figure 7C). As expected, after 24 hours of loading, mice from both genotypes were already at steady state and exhibited the same alkaline urine pH values and the same bicarbonate excretion. The defect in renal bicarbonate excretion is likely to be the consequence of abnormal bicarbonate secretion and not of decreased filtration, since glomerular filtration rate per body mass in *IRR*$^{-/-}$ and *IRR*$^{+/+}$ mice was measured as identical (Figure S6C).

Renal adaptation to an alkaline-load implies an increase in bicarbonate secretion by beta-intercalated cells of the collecting duct. This adaptation is supported by increased expression of the apical Cl^-/HCO_3^- exchanger pendrin (Wagner et al., 2002). To confirm that IRR disruption affects β-IC, we measured the abundance of pendrin and of the B1 subunit of the V-H^+-ATPase in the kidney cortex of alkali-loaded *IRR*$^{-/-}$ and WT mice by Western blot. Even though *IRR*$^{-/-}$ mice exhibited a much more marked metabolic alkalosis following alkaline-loading (Figure 7B), and hence, were expected to exhibit increased pendrin and proton pump abundance, they showed ~40% decrease in both protein abundance when compared to *IRR*$^{+/+}$ mice indicating that IRR disruption impairs the capability of the collecting duct to adapt to alkalosis (Figure 7D).

DISCUSSION

Our attempts to identify an endogenous ligand of IRR, a close homolog of IR and IGF-IR that both have peptide agonists, led to the unexpected observation that IRR is activated by mildly alkaline extracellular pH, a substance of a non-peptide nature. Moreover, *in vivo* experiments demonstrated that IRR is required for normal adaptation of collecting duct in response to metabolic alkalosis. Thus, we propose that IRR functions as a pH sensing receptor.

The activation of IRR by hydroxyl anion resembles canonical receptor-ligand interaction. Firstly, it is concentration dependent, with a characteristic saturation curve, and fully reversible. Secondly, it is specific; two closely homologous receptors IR and IGF-IR, as well as another receptor tyrosine kinase EGFR, are not activated by alkaline media. Thirdly, the pH-sensing property of IRR is determined solely by the structure of its extracellular domain. Like with other cell surface receptors, IRR activation by alkali triggers a conformational change in the receptor molecule, stimulates intracellular signaling (involving IRS-1 and AKT/PKB) and results in cytoskeleton rearrangement. The absence of IRR basal autophosphorylation together with the estimated pH dependence of IRR activation suggest that the hydroxyl anion is possibly its only natural agonist and the receptor remains silent within the regular homeostasis range (pH 7.2–7.6) of blood and interstitial fluid. Whereas an alkali-sensing ion channel has been described previously (Niemeyer et al., 2007), IRR is the first example of the metabotropic-type receptor that can be activated by mildly alkaline media.

All of the previously identified receptor tyrosine kinase ligands are proteins that activate the receptors by induction of their dimerization. In the unique case of the insulin receptor family the subunits are pre-dimerized by disulfide bonds and require allosteric activation by a ligand. 3D structures of the first three domains (L1–F–L2) of IR (Lou et al., 2006) and IGF-IR (Ward et al., 2001), as well as the whole IR ectodomain structure (McKern et al., 2006) revealed possible mechanisms of insulin and IGF capture by their receptors, and also uncovered a quite unexpected Λ-shape of the IR ectodomain (a.k.a. "folded-over conformation"). These structures delineated the insulin binding to two receptor sites: site-1, lying on the surface of the central β-sheet of L1 domain in one of disulfide-linked monomers of the receptor, and site-2 at the junction of FnIII-1 and FnIII-2 of the opposite monomer. Yet another, symmetrical, ligand binding site that is capable of binding another insulin molecule is formed by FnIII-1/2 of the second monomer and L1 of the first one. Insulin is proposed first to interact with the low affinity site, and then "crosslink" the receptor dimer by contacting with the second site in the opposite monomer, which creates the high-affinity site. This conformational change of the receptor is thought to be the origin of negative cooperativity (Lawrence et al., 2007), since when the primary ligand binding site is occupied, the affinity at the symmetrical site simultaneously drops (De Meyts, 2008).

Agonist of IRR — hydroxyl ion — is a small molecule and cannot exhibit simultaneous interactions with symmetrical receptor subunits like insulin does. We found that, in contrast with IR activation, IRR shows strong positive cooperativity in response to pH (Hill coefficient 3.5±0.5), suggesting that several sites in the receptor molecule, primarily located in the first two domains – L1 and F – of its extracellular region, are involved in alkali-sensing and react with each next hydroxyl ion more readily than the previous. Another interesting possibility to be tested is that activated IRR forms oligomers.

We can speculate that IRR pH sensitivity in 7.9–9.2 range could be determined by several amino acid residues with ionogenic groups of its ectodomain. Cysteines have close pKa about 8.5 but they presumably exist as oxidized Cys-Cys bridges within and between receptor ectodomains as shown for homologous IR (Sparrow et al., 1997) but perhaps deserving additional tests in the case of IRR. The role of other amino acid residues such as histidines (pKa 6.5), tyrosines (pKa 10), lysines (pKa 10) and even arginines (pKa 12) is quite possible since protein microenvironment may significantly alter amino acid residue pKa values (Srivastava et al., 2007).

The proposed physiological role of IRR as a pH sensor correlates well with the known pattern of IRR distribution. In our *in vitro* experiments, robust phosphorylation of IRR was detectable at pH 7.9, a value that exceeds the general physiological range. However, the tissues that harbor IRR are characteristic for direct contacts with extracorporal media of extreme pH. Largest concentrations of IRR are found in the kidney where it is restricted to B type intercalated tubular cells (β-IC) (Bates et al., 1997; Ozaki et al., 1997), a subpopulation of renal epithelial cells that control renal excretion of base. IRR is also expressed in stomach enterochromaffin-like cells (Tsujimoto et al., 1995). These cells are located close to the stomach lining in the alkaline protective barrier and their function is to secrete histamine, a paracrine factor that modulates gastric acid secretion. Importantly, acid secretion by the stomach is paralleled by a massive efflux of bicarbonate into the extracellular medium surrounding the stomach epithelium, a phenomenon also known as the alkaline tide phenomenon (Niv and Fraser, 2002). In the pancreas, IRR is found in pancreatic beta-cells (Ozaki, 1998) that can face the duct lumen containing pancreatic juice with typical pH 8.0–8.5 and regulate bicarbonate secretion from the duct cells as the function of extracellular pH (Bertelli and Bendayan, 2005). Yet, in the nervous tissue cells, where IRR co-expresses with TrkA, its close chromosome neighbor sharing regulatory elements (Ma et al., 2000), extracellular pH reportedly cannot exceed 7.8 (Chesler, 2003) that would prevent IRR from

activation. Therefore, its gene proximity-driven co-expression with TrkA may be either serendipitous or rudimentary that has not been eliminated by the evolutionary pressure.

As noted above, IRR is primarily expressed in kidney β-IC cells that mediate net base secretion (or acid absorption) in response to an alkali load, or to metabolic alkalosis. β-IC cells are characterized by the presence of an apical Cl^-/HCO_3^- exchanger pendrin (pds, Slc26a4) and a basolateral vacuolar H^+-ATPase (Royaux et al., 2001). Another intercalated cell type, called α-IC, exhibit same acid-base transport properties but with the opposite polarization. Indeed, α-IC harbor a basolateral Cl^-/HCO_3^- exchanger and an apical v-H^+-ATPase (Wall, 2005). As a consequence, α-IC mediate net acid secretion (or base absorption). Depending on the conditions, the collecting duct can adapt rapidly from a state in which it does secrete acid, to another state in which it does secrete base (Schwartz et al., 1985). Importantly, it has been shown that exposure of isolated collecting duct to an acidic medium stimulates acid secretion, and, that the same tubule can revert its transport activity from proton to bicarbonate secretion if it is subsequently exposed to alkaline media (Purkerson et al., 2010).

These studies indicate that intercalated cells are able to “sense” the pH of the extracellular fluid, and adapt their activity in the absence of any endocrine control.

We postulated that since IRR is a pH sensor activated by changes of extracellular pH toward alkaline value, it might be involved in the signaling pathway that triggers activation of bicarbonate secretion by IRR-expressing renal β-IC cells in response to alkali loading. In support of this hypothesis, we found that IRR disruption impaired renal adaptation to alkali loading since *IRR*$^{-/-}$ mice developed metabolic alkalosis in response to this challenge. Moreover, this effect was related to the inability to increase pendrin expression, demonstrating that IRR is required for normal adaptation of the collecting duct to alkalosis.

EXPERIMENTAL PROCEDURES

Full-length cDNA clones of human IR, IGF-IR, and IRR were assembled from a commercially available EST clones (I.M.A.G.E.) and fully verified by sequencing. Coding sequences of all receptor clones were in agreement with the corresponding GenBank entries with accession numbers NM_000208, NM_000875 and NM_014215. The cDNA clone of *Xenopus laevis* IRR was obtained from OpenBioSystem (clone ID 4031728). To generate HA epitope-tagged receptors, the receptor sequences were fused by PCR to the C-terminal nucleotide sequence encoding influenza hemagglutinin epitope tag (YPYDVPDYA) and subcloned into mammalian expression vector pcDNA3 (Invitrogen). Construction of IRR/IR mutants is described in the Supplement.

Transfections and analysis of receptor tyrosine kinase activation in cell cultures

CHO cells were cultured in F-12 medium supplemented with 10% fetal bovine serum (Hyclone), 1% penicillin/streptomycin, 2 mM L-glutamine. The COS, HEK 293, HeLa and A431 cells were cultured in DMEM supplemented with 10% fetal bovine serum (Hyclone), 1% penicillin/streptomycin, 2 mM L-glutamine. MIN6 cells were cultured in DMEM supplemented with 10% fetal bovine serum (Hyclone), 1% penicillin/streptomycin, 2 mM L-glutamine, 0.11 mg/l pyruvate, and 30 μM β-mercaptoethanol.

CHO and HEK 293 cells were transfected by unifectin-56 according to the manufacturer’s protocol (Unifect Group, Russia). For selection of stably transfected clones, the cells were grown in the medium with added G418 antibiotic (Sigma, 600 μg/ml). Three independent IRR-overexpressing CHO cell lines were obtained with variable IRR expression but the same receptor properties with regards to the alkali stimulation.

In autophosphorylation assays, confluent monolayers of cells culture dishes were washed by serum-free F-12 and incubated overnight in serum-free F-12 containing 1% penicillin/streptomycin. The serum-starved cells were incubated with assayed media for 10 min at room temperature or at 37°C and solubilized in the lysis buffer (50 mM Tris-HCl, pH 7.5, 150 mM NaCl, 0.5% NP-40, 1% Triton X-100, 0.5 mM EDTA, 0.5 mM EGTA, 10% glycerol, 0.5 mM phenylmethylsulphonyl fluoride, 1 mM Na_3VO_4, 1:100 (v/v) protease inhibitor cocktail (P8340, Sigma)) for 10 min on ice. Receptor tyrosine kinase activation was assessed by SDS-eletrophoresis of lysed cells or immunoprecipitates followed by Western blotting and ECL detection by SuperSignal kits (Pierce), essentially as described (Deyev and Petrenko, 2010). The utilized antibodies are described in the Supplement.

Activation of IRR in intact kidney under alkali load

The abdominal cavity of anesthetized rat was opened and a polyethylene (PE-50) catheter was implanted into the abdominal aorta via femoral artery so that the tip of catheter reached renal arteries. 1% $NaHCO_3$ solution was injected via catheter at a volume of 1 ml/100 g of body weight gradually, with 1 min intervals. A control animal was injected with appropriate volume of 0.9% NaCl. Urine was collected at 10-minute intervals by urinary bladder syringe puncture and immediately transferred into vial for pH measuring with a microelectrode or test stripes. On reaching of urine pH>8.3, the kidneys were immediately excised and homogenized in 30 ml of 20 mM Hepes pH 7.4, 10 mM EDTA, 3 mM Na_3VO_4, 1:100 (v/v) protease inhibitor cocktail (P8340, Sigma) in a glass-teflon homogenizer. The crude membrane fraction was obtained by centrifugation for 30 min at 30,000g and extracted with 25 ml of 20 mM Hepes pH 7.4, 150 mM NaCl, 1% Triton X-100, 10 mM EDTA, 3 mM Na_3VO_4, and 1:100 (v/v) protease inhibitor cocktail. The insoluble material was removed by centrifugation for 30 min at 50,000g and the obtained supernatant was filtered through 0.45 μm filter. IRR was immunoprecipitated with 8 μg of purified anti-rIRR antibody or rabbit IgG (Imtek, Russia) from 6 ml of the extract and further analyzed by Western blotting.

IRR knock-out mice analyses

IRR$^{-/-}$ mice were obtained by fertilization of C57BL6 wild type mice with frozen sperm of *IRR*$^{-/-}$, *IR*$^{-/+}$, *IGF-IR*$^{-/+}$ mice (Nef et al., 2003). After more than 8 cycles of breeding along with PCR genotyping, *IRR*$^{-/-}$ mice line of specific pathogen free (SPF) status on a pure C57Bl6 genetic background was isolated.

All experiments were performed using age- and sex-matched *IRR*$^{-/-}$ and wild type C57Bl6 mice (4 months old). Mice were given deionized water *ad libitum*, pair-fed with standard laboratory chow containing 0.3% of sodium (INRA, France), and were housed at constant room temperature (24 ± 1°C) with 12-hour light/dark cycle. Urine collections were performed on mice kept in metabolic cages (Techniplast, France) in order to be able to verify accuracy of the pair feeding and to check that the volume of drinking solution was exactly identical between groups. Mice were first acclimatized for 4–5 days with a free access to deionized water and standard laboratory mice chow. Then experiments started at 9 a.m. after voiding the bladder by massage. Urine was collected by bladder massage at 3 p.m. (6 hours after the experiment started) and after 24 hours to measure pH and bicarbonate urinary excretion. On the second day, drinking water was replaced by 0.28M $NaHCO_3$ solution and collections were repeated with the exactly same timing. This treatment has been shown previously by us to induce a mild metabolic alkalosis and to stimulate renal bicarbonate excretion in rats (Eladari et al., 2002; Quentin et al., 2004b) and same effects have been described in mice by others (Wagner et al., 2002). All the urine were collected under mineral oil to avoid CO_2 evaporation and samples were analyzed immediately.

To test chronic effects of alkaline loading on acid-base status of the animals, awake untreated mice were first sampled by retro-orbital puncture and blood gas was analyzed, then mice were allowed to recover during two weeks before starting alkaline loading with 0.28M $NaHCO_3$ drinking solution. To check that the effects observed after $NaHCO_3$ loading did not result from the sodium load, a control group consisted of $IRR^{-/-}$ or wild type mice that were given 0.28M NaCl drinking solution instead of 0.28M $NaHCO_3$. After 7 days of loading, the mice were sampled and blood gas was analyzed again. Then mice were sacrificed and kidneys were removed for Western blot analyses of pendrin and Atp6v1b1 protien abundance. Urine and blood pH and bicarbonate concentration were measured using a pH/blood-gas analyzer (ABL 725, Radiometer, Copenhagen, Denmark).

Highlights

Insulin receptor-related receptor (IRR) is activated at pH>7.9.

IRR activation is dose-dependent, positively cooperative and quickly reversible.

IRR pH sensitivity is primarily defined by its L1F extracellular domains.

IRR function in the kidney is coupled to bicarbonate secretion.

Supplementary Material

Refer to Web version on PubMed Central for supplementary material.

Acknowledgments

We are grateful to Dr. Qais Al-Awqati for helpful comments on our project and valuable advice regarding acid-base physiology. We thank Drs. Joseph Schlessinger and Alexander Gabibov for critically reading the manuscript, their continuous support and advice, and Ms. Valentina Petrenko for carefully editing the manuscript. We are indebted to Drs. S. Nef & L. Parada (UT Southwestern Medical Center, Dallas) for providing the frozen sperm of IRR/IR/IGFIR knockout mice and Dr. Gregory Enikolopov (Cold Spring Harbor Laboratory) for granting support for *in vitro* fertilization. This project was supported by Molecular and Cellular Biology Program of the Russian Academy of Sciences (to AGP and NNN), Russian Foundation for Basic Research (to IED), by Basic Sciences to Medicine Program of the Russian Academy of Sciences and by NIH Fogarty grant 5 RO3 TW007210 (to AGP), TNH from the Fondation Leducq, grants PHYSIO 2007-RPV07084, ANR BLANC 2010-R10164DD (to DE), and ANR-07-PHYSIO-027 (to PH) from l'Agence Nationale de la Recherche.

References

Bates CM, Merenmies JM, Kelly-Spratt KS, Parada LF. Insulin receptor-related receptor expression in non-A intercalated cells in the kidney. Kidney international. 1997; 52:674–681. [PubMed: 9291186]

Bertelli E, Bendayan M. Association between endocrine pancreas and ductal system. More than an epiphenomenon of endocrine differentiation and development? J Histochem Cytochem. 2005; 53:1071–1086. [PubMed: 15956021]

Chesler M. Regulation and modulation of pH in the brain. Physiol Rev. 2003; 83:1183–1221. [PubMed: 14506304]

Dandekar AA, Wallach BJ, Barthel A, Roth RA. Comparison of the signaling abilities of the cytoplasmic domains of the insulin receptor and the insulin receptor-related receptor in 3T3-L1 adipocytes. Endocrinology. 1998; 139:3578–3584. [PubMed: 9681510]

De Meyts P. Insulin and insulin-like growth factors: the paradox of signaling specificity. Growth Horm IGF Res. 2002; 12:81–83. [PubMed: 12175644]

De Meyts P. The insulin receptor: a prototype for dimeric, allosteric membrane receptors? Trends in biochemical sciences. 2008; 33:376–384. [PubMed: 18640841]

Deyev IE, Petrenko AG. Regulation of CIRL-1 proteolysis and trafficking. Biochimie. 2010; 92:418–422. [PubMed: 20100540]

Dissen GA, Garcia-Rudaz C, Tapia V, Parada LF, Hsu SY, Ojeda SR. Expression of the Insulin Receptor-Related Receptor (IRR) is Induced by the Preovulatory Surge of LH in Thecal-Interstitial Cells of the Rat Ovary. Endocrinology. 2005

Dupont J, LeRoith D. Insulin and insulin-like growth factor I receptors: similarities and differences in signal transduction. Horm Res. 2001; 55 Suppl 2:22–26. [PubMed: 11684871]

Eladari D, Leviel F, Pezy F, Paillard M, Chambrey R. Rat proximal NHE3 adapts to chronic acid-base disorders but not to chronic changes in dietary NaCl intake. Am J Physiol Renal Physiol. 2002; 282:F835–F843. [PubMed: 11934693]

Florke RR, Schnaith K, Passlack W, Wichert M, Kuehn L, Fabry M, Federwisch M, Reinauer H. Hormone-triggered conformational changes within the insulin-receptor ectodomain: requirement for transmembrane anchors. The Biochemical journal. 2001; 360:189–198. [PubMed: 11696007]

Hernandez-Sanchez C, Mansilla A, de Pablo F, Zardoya R. Evolution of the insulin receptor family and receptor isoform expression in vertebrates. Molecular biology and evolution. 2008; 25:1043–1053. [PubMed: 18310661]

Hirayama I, Tamemoto H, Yokota H, Kubo SK, Wang J, Kuwano H, Nagamachi Y, Takeuchi T, Izumi T. Insulin receptor-related receptor is expressed in pancreatic beta-cells and stimulates tyrosine phosphorylation of insulin receptor substrate-1 and −2. Diabetes. 1999; 48:1237–1244. [PubMed: 10342810]

Jui HY, Suzuki Y, Accili D, Taylor SI. Expression of a cDNA encoding the human insulin receptor-related receptor. The Journal of biological chemistry. 1994; 269:22446–22452. [PubMed: 8071374]

Kanzaki M. Insulin receptor signals regulating GLUT4 translocation and actin dynamics. Endocrine journal. 2006; 53:267–293. [PubMed: 16702775]

Kelly-Spratt KS, Klesse LJ, Merenmies J, Parada LF. A TrkB/insulin receptor-related receptor chimeric receptor induces PC12 cell differentiation and exhibits prolonged activation of mitogen-activated protein kinase. Cell Growth Differ. 1999; 10:805–812. [PubMed: 10616905]

Kelly-Spratt KS, Klesse LJ, Parada LF. BDNF activated TrkB/IRR receptor chimera promotes survival of sympathetic neurons through Ras and PI-3 kinase signaling. J Neurosci Res. 2002; 69:151–159. [PubMed: 12111796]

Kitamura T, Kido Y, Nef S, Merenmies J, Parada LF, Accili D. Preserved pancreatic beta-cell development and function in mice lacking the insulin receptor-related receptor. Mol Cell Biol. 2001; 21:5624–5630. [PubMed: 11463843]

Klammt J, Garten A, Barnikol-Oettler A, Beck-Sickinger AG, Kiess W. Comparative analysis of the signaling capabilities of the insulin receptor-related receptor. Biochem Biophys Res Commun. 2005; 327:557–564. [PubMed: 15629149]

Kristensen C, Wiberg FC, Andersen AS. Specificity of insulin and insulin-like growth factor I receptors investigated using chimeric mini-receptors. Role of C-terminal of receptor alpha subunit. The Journal of biological chemistry. 1999; 274:37351–37356. [PubMed: 10601304]

Lawrence MC, McKern NM, Ward CW. Insulin receptor structure and its implications for the IGF-1 receptor. Current opinion in structural biology. 2007; 17:699–705. [PubMed: 17851071]

Lou M, Garrett TP, McKern NM, Hoyne PA, Epa VC, Bentley JD, Lovrecz GO, Cosgrove LJ, Frenkel MJ, Ward CW. The first three domains of the insulin receptor differ structurally from the insulin-like growth factor 1 receptor in the regions governing ligand specificity. Proceedings of the National Academy of Sciences of the United States of America. 2006; 103:12429–12434. [PubMed: 16894147]

Ma L, Merenmies J, Parada LF. Molecular characterization of the TrkA/NGF receptor minimal enhancer reveals regulation by multiple cis elements to drive embryonic neuron expression. Development. 2000; 127:3777–3788. [PubMed: 10934022]

Mathi SK, Chan J, Watt VM. Insulin receptor-related receptor messenger ribonucleic acid: quantitative distribution and localization to subpopulations of epithelial cells in stomach and kidney. Endocrinology. 1995; 136:4125–4132. [PubMed: 7649121]

McKern NM, Lawrence MC, Streltsov VA, Lou MZ, Adams TE, Lovrecz GO, Elleman TC, Richards KM, Bentley JD, Pilling PA, Hoyne PA, Cartledge KA, Pham TM, Lewis JL, Sankovich SE, Stoichevska V, Da Silva E, Robinson CP, Frenkel MJ, Sparrow LG, Fernley RT, Epa VC, Ward

CW. Structure of the insulin receptor ectodomain reveals a folded-over conformation. Nature. 2006; 443:218–221. [PubMed: 16957736]

Nef S, Verma-Kurvari S, Merenmies J, Vassalli JD, Efstratiadis A, Accili D, Parada LF. Testis determination requires insulin receptor family function in mice. Nature. 2003; 426:291–295. [PubMed: 14628051]

Niemeyer MI, Gonzalez-Nilo FD, Zuniga L, Gonzalez W, Cid LP, Sepulveda FV. Neutralization of a single arginine residue gates open a two-pore domain, alkali-activated K+ channel. Proceedings of the National Academy of Sciences of the United States of America. 2007; 104:666–671. [PubMed: 17197424]

Niv Y, Fraser GM. The alkaline tide phenomenon. Journal of clinical gastroenterology. 2002; 35:5–8. [PubMed: 12080218]

Ozaki K. Insulin receptor-related receptor in rat islets of Langerhans. Eur J Endocrinol. 1998; 139:244–247. [PubMed: 9724084]

Ozaki K, Takada N, Tsujimoto K, Tsuji N, Kawamura T, Muso E, Ohta M, Itoh N. Localization of insulin receptor-related receptor in the rat kidney. Kidney international. 1997; 52:694–698. [PubMed: 9291189]

Purkerson JM, Tsuruoka S, Suter DZ, Nakamori A, Schwartz GJ. Adaptation to metabolic acidosis and its recovery are associated with changes in anion exchanger distribution and expression in the cortical collecting duct. Kidney international. 2010; 78:993–1005. [PubMed: 20592712]

Quentin F, Chambrey R, Trinh-Trang-Tan MM, Fysekidis M, Cambillau M, Paillard M, Aronson PS, Eladari D. The Cl-/HCO3- exchanger pendrin in the rat kidney is regulated in response to chronic alterations in chloride balance. Am J Physiol Renal Physiol. 2004a; 287:F1179–F1188. [PubMed: 15292050]

Quentin F, Eladari D, Frische S, Cambillau M, Nielsen S, Alper SL, Paillard M, Chambrey R. Regulation of the Cl-/HCO3- exchanger AE2 in rat thick ascending limb of Henle's loop in response to changes in acid-base and sodium balance. J Am Soc Nephrol. 2004b; 15:2988–2997. [PubMed: 15579501]

Renteria ME, Gandhi NS, Vinuesa P, Helmerhorst E, Mancera RL. A comparative structural bioinformatics analysis of the insulin receptor family ectodomain based on phylogenetic information. PloS one. 2008; 3:e3667. [PubMed: 18989367]

Royaux IE, Wall SM, Karniski LP, Everett LA, Suzuki K, Knepper MA, Green ED. Pendrin, encoded by the Pendred syndrome gene, resides in the apical region of renal intercalated cells and mediates bicarbonate secretion. Proceedings of the National Academy of Sciences of the United States of America. 2001; 98:4221–4226. [PubMed: 11274445]

Sabolic I, Brown D, Gluck SL, Alper SL. Regulation of AE1 anion exchanger and H(+)-ATPase in rat cortex by acute metabolic acidosis and alkalosis. Kidney international. 1997; 51:125–137. [PubMed: 8995726]

Schwartz GJ, Barasch J, Al-Awqati Q. Plasticity of functional epithelial polarity. Nature. 1985; 318:368–371. [PubMed: 2415824]

Shier P, Watt VM. Primary structure of a putative receptor for a ligand of the insulin family. The Journal of biological chemistry. 1989; 264:14605–14608. [PubMed: 2768234]

Sparrow LG, McKern NM, Gorman JJ, Strike PM, Robinson CP, Bentley JD, Ward CW. The disulfide bonds in the C-terminal domains of the human insulin receptor ectodomain. The Journal of biological chemistry. 1997; 272:29460–29467. [PubMed: 9368005]

Srivastava J, Barber DL, Jacobson MP. Intracellular pH sensors: design principles and functional significance. Physiology (Bethesda, Md. 2007; 22:30–39.

Tsujimoto K, Tsuji N, Ozaki K, Ohta M, Itoh N. Insulin receptor-related receptor messenger ribonucleic acid in the stomach is focally expressed in the enterochromaffin-like cells. Endocrinology. 1995; 136:558–561. [PubMed: 7835288]

Ullrich A, Bell JR, Chen EY, Herrera R, Petruzzelli LM, Dull TJ, Gray A, Coussens L, Liao YC, Tsubokawa M, et al. Human insulin receptor and its relationship to the tyrosine kinase family of oncogenes. Nature. 1985; 313:756–761. [PubMed: 2983222]

Ullrich A, Gray A, Tam AW, Yang-Feng T, Tsubokawa M, Collins C, Henzel W, Le Bon T, Kathuria S, Chen E, et al. Insulin-like growth factor I receptor primary structure: comparison with insulin

receptor suggests structural determinants that define functional specificity. Embo J. 1986; 5:2503–2512. [PubMed: 2877871]

Wagner CA, Finberg KE, Stehberger PA, Lifton RP, Giebisch GH, Aronson PS, Geibel JP. Regulation of the expression of the Cl-/anion exchanger pendrin in mouse kidney by acid-base status. Kidney international. 2002; 62:2109–2117. [PubMed: 12427135]

Wall SM. Recent advances in our understanding of intercalated cells. Curr Opin Nephrol Hypertens. 2005; 14:480–484. [PubMed: 16046908]

Ward CW, Garrett TP, McKern NM, Lou M, Cosgrove LJ, Sparrow LG, Frenkel MJ, Hoyne PA, Elleman TC, Adams TE, Lovrecz GO, Lawrence LJ, Tulloch PA. The three dimensional structure of the type I insulin-like growth factor receptor. Mol Pathol. 2001; 54:125–132. [PubMed: 11376122]

Zhang B, Roth RA. The insulin receptor-related receptor. Tissue expression, ligand binding specificity, and signaling capabilities. The Journal of biological chemistry. 1992; 267:18320–18328. [PubMed: 1326521]

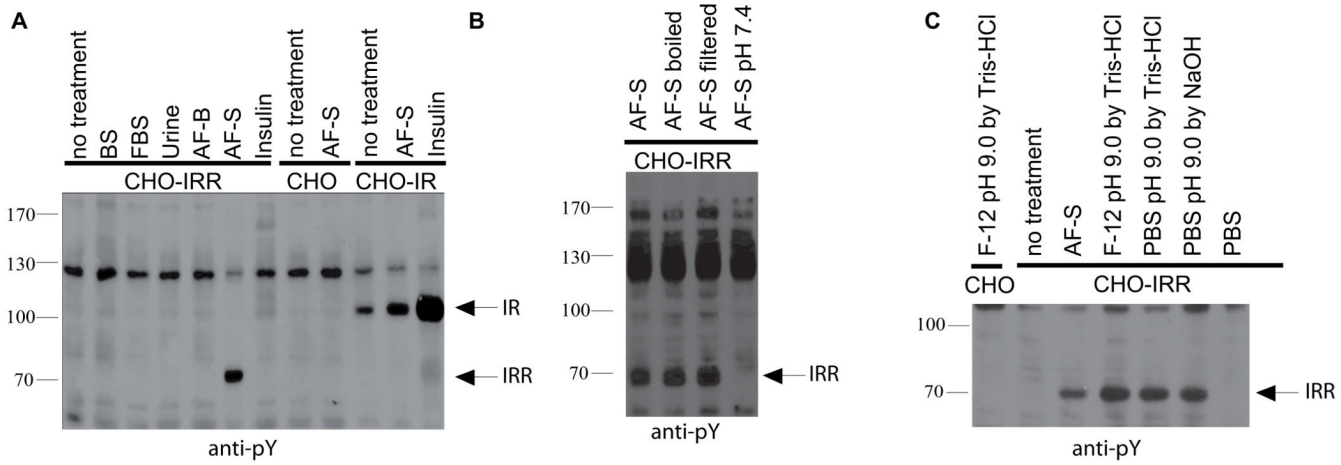

Figure 1. Activation of IRR in transfected cells

(A) Fluids stimulation of tyrosine phosphorylation in CHO-IR and CHO-IRR cells. The starved cells were incubated with 10% of indicated fluids or 1 μM insulin in F-12 media for 10 min, lysed and analyzed by Western blotting with anti-pY antibody. BS – bovine serum, FBS – fetal bovine serum, AF-B – bovine amniotic fluid (Biolot, Russia), AF-S -bovine amniotic fluid (Sigma, USA), PBS – phosphate-buffered saline. (B) Characteristics of the IRR activation. The sample of amniotic fluid was boiled for 5 min, or filtered through a 10,000 Da cut-off membrane, or adjusted to pH 7.4 with Tris-HCl and tested as in (A). (C) Stimulation of CHO-IRR cells with alkaline media. The CHO and CHO-IRR cells were incubated for 10 min with indicated media and analyzed as in (A). All Western blots shown are representative of at least 3 independent experiments.

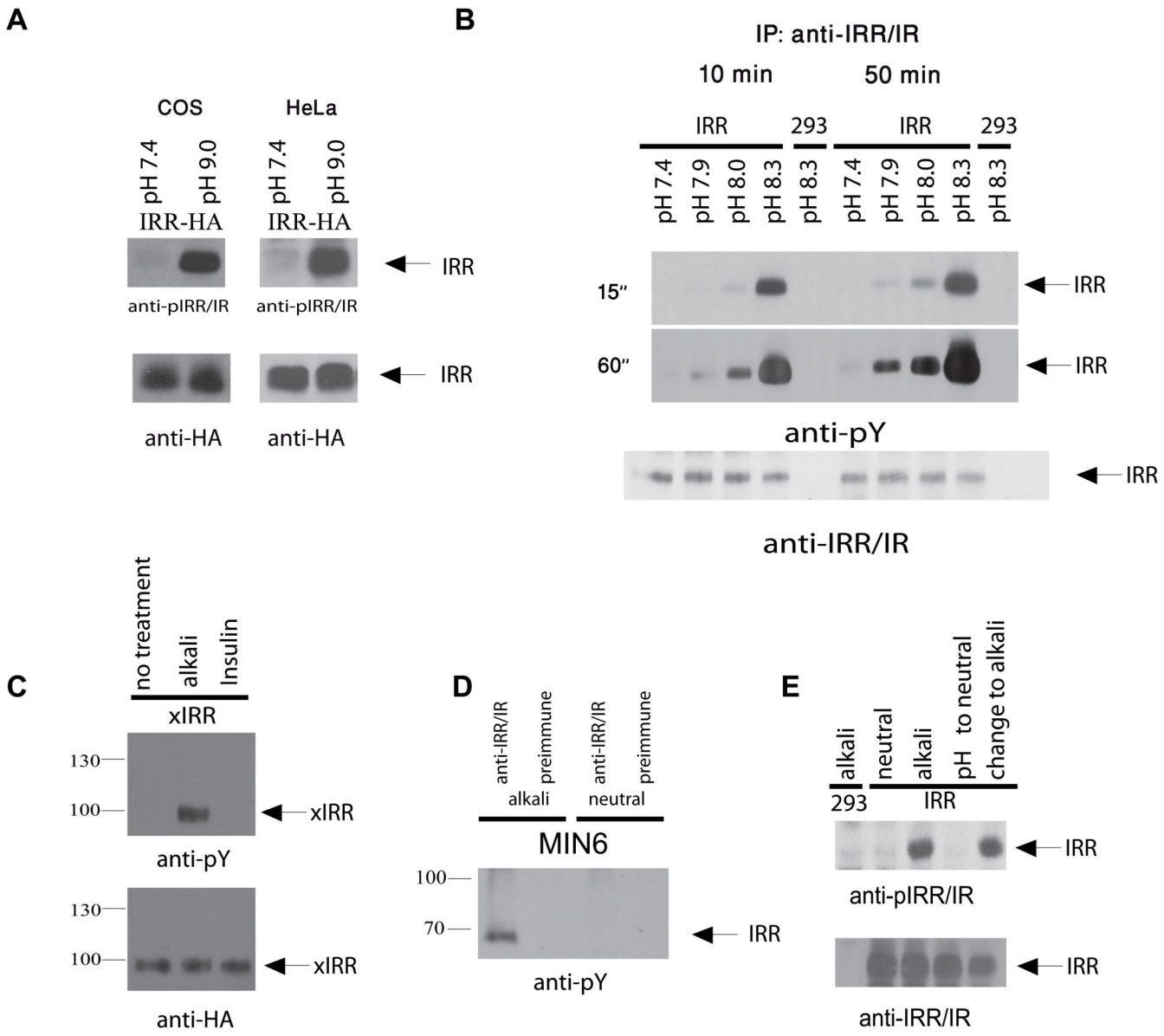

Figure 2. IRR can be activated by mildly alkaline media

(A) COS and HeLa cells, transfected with IRR, were treated with neutral and alkaline media, then lysed and blotted with anti-pIRR/IR or anti-HA antibodies. (B) IRR-transfected HEK 293 cells were incubated for 10 or 50 min in PBS media, adjusted to the indicated pH with 60 mM EPPS; the cells were then lysed, immunoprecipitated with anti-IRR/IR antibodies, and blotted with anti-pY (two ECL exposure times of the same blot are shown on the left) or anti-IRR/IR antibodies. Semiquantitative densitometry is shown on Figure S1B. (C) Activation of IRR from *Xenopus laevis* (xIRR) by alkali. HEK 293 cells were transfected with xIRR expression plasmid. After starvation, cells were incubated for 10 min in PBS, adjusted to pH 9.0 by Tris-HCl, or with 1μM insulin. The cells were then lysed and immunoprecipitated with anti-HA-agarose. The precipitates were stained with anti-pY or anti-HA antibodies. β-subunit bands are indicated by arrows. (D) Activation of endogenous IRR in MIN6 cells. Serum-starved MIN6 cells were incubated for 10 min in PBS pH 7.4 or PBS adjusted to pH 9.0. The cells were lysed and immunoprecipitated with anti-IRR/IR

antibody or pre-immune serum, and blotted with anti-pY antibody. (E) Reversibility of IRR activation after extensive washes. HEK 293 cells transfected with IRR were incubated with PBS pH 9.0, then washed extensively with PBS pH 7.4, and treated again with PBS pH 9.0 (see the Supplement for details). Cell lysates were blotted with anti-pIRR/IR and anti-IRR/IR antibodies. All Western blots shown are representative of at least 3 independent experiments. See also Figure S1.

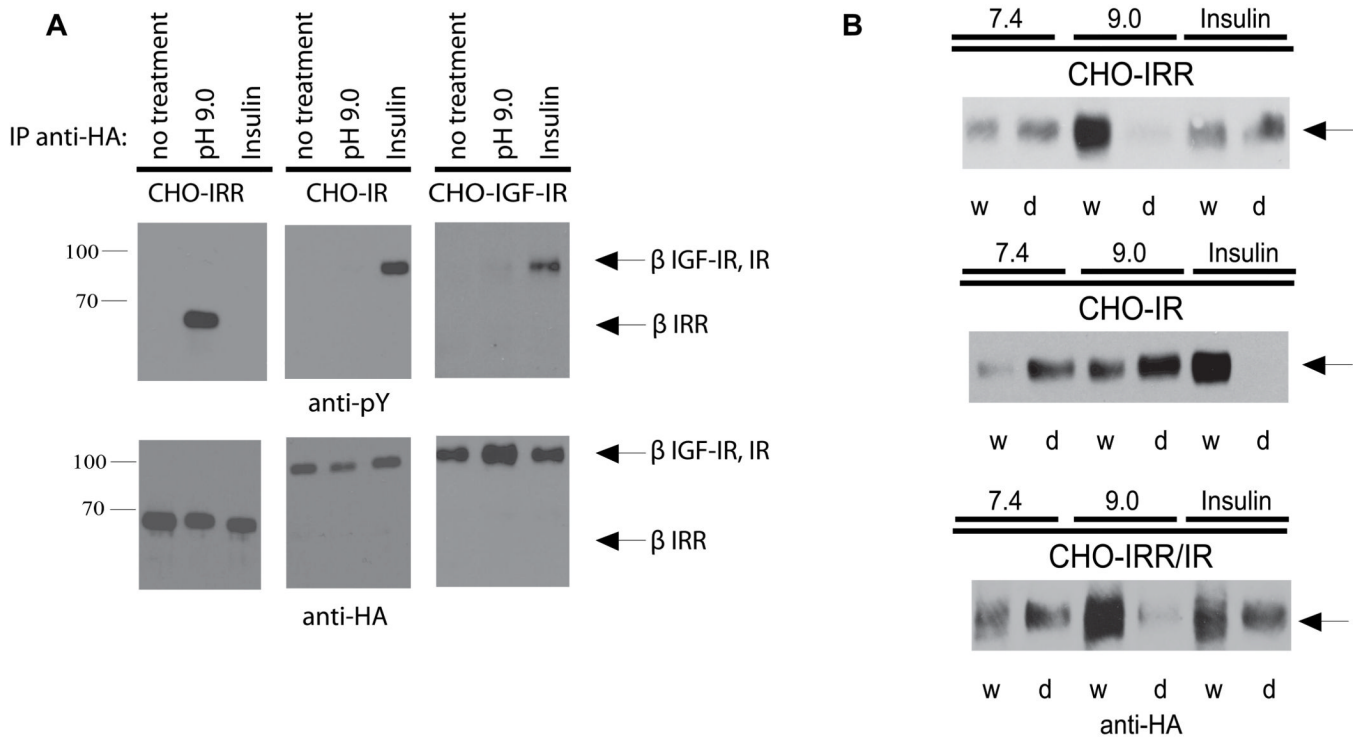

Figure 3. Specificity and structural response to IRR activation by alkali

(A) Activation of IRR but not of IR and IGF-IR by alkali. After starvation, the indicated stably transfected cell lines were incubated for 10 min in PBS adjusted to pH 9.0 or with 1 μM insulin. Cells were then lysed, immunoprecipitated with anti-HA antibody, and Western blotted with anti-pY or anti-HA antibody. (B) Analysis of IRR, IR and IRR/IR chimera conformational changes by the detergent phase distribution assay. Non-starved stably transfected CHO cells were lysed in Triton X-114 containing buffers adjusted to pH 7.4 or 9.0, or supplemented with 0.5 μM insulin, and analyzed by detergent phase distribution (Florke et al., 2001), as described in detail in Supplemental Experimental Procedures. Equal aliquots of the separated phases (w – detergent-depleted, d – detergent enriched) were Western blotted with anti-HA antibody to determine receptor concentration. See also Figure S2.

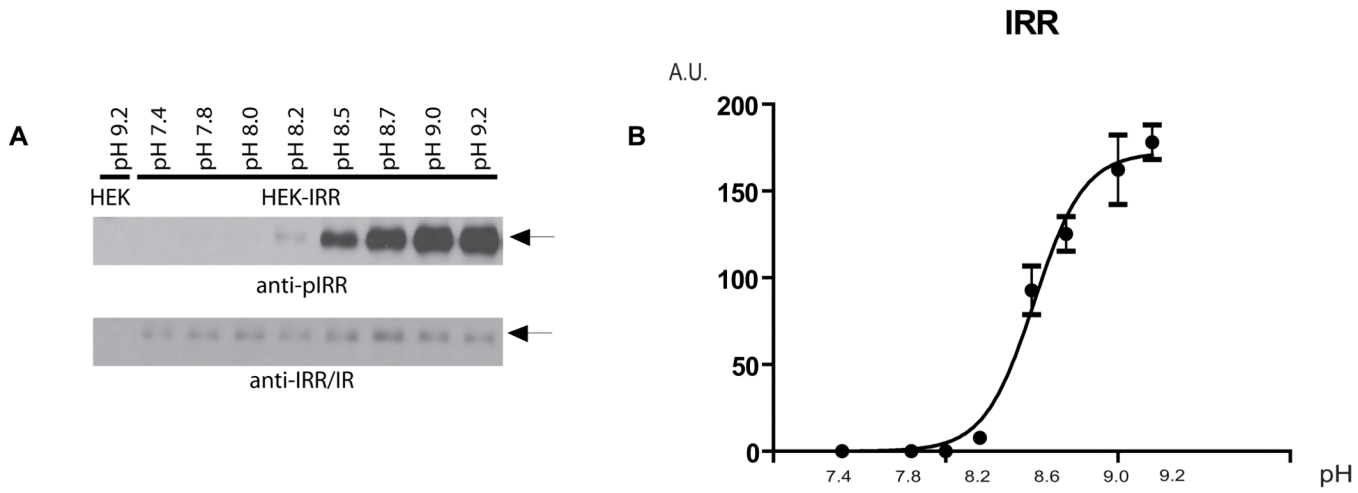

Figure 4. pH-dependence of IRR activation

(A) Non-starved IRR-transfected HEK 293 cells were incubated for 10 min with PBS medium adjusted to the indicated pH by 60 mM Tris-HCl buffer, then lysed and blotted with anti-pIRR/IR and anti-IRR/IR antibodies. Western blot images representative of four independent experiments are shown. (B) The Western blot images were scanned in the area of the IRR β-subunit band and the integrated optical density of the anti-pIRR/IR images, normalized by the anti-IRR/IR density, was plotted v.s. pH of the tested solutions. Values are means ± SE (n=4). β-subunit bands are indicated by arrows. See also Figure S3.

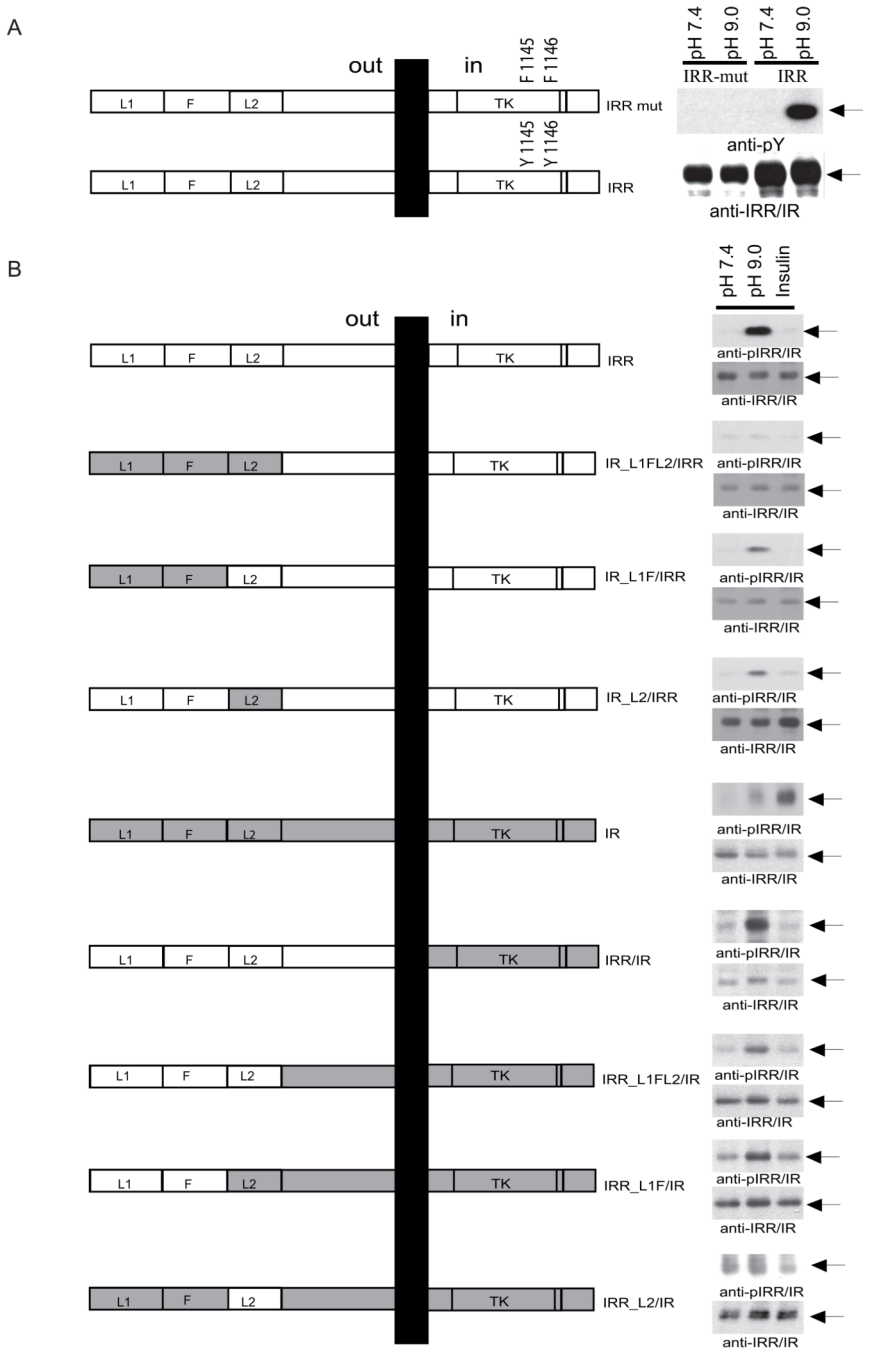

Figure 5. Structural determinants of IRR activation

(A) Inhibition of IRR activation by tyrosine mutations (IRR mut) in the catalytic domain (left panel). HEK 293 cells were transfected with HA-tagged IRR and mutated IRR. After 24 hrs growth, the cells were starved for 12 hrs, and then incubated for 10 min in PBS medium at pH 7.4 or 9.0. Cell lysates were analyzed by Western blotting with anti-pY or anti-IRR/IR antibodies (right panel). β-subunit bands are indicated by arrows. (B) Domain models of the HA-tagged IRR/IR. L – receptor L domain, F – furin-like repeats, TK – catalytic tyrosine-kinase domain. Right panel shows activation of IRR/IR chimeras by alkali or insulin. HEK 293 cells transfected with the indicated chimeras were treated with F-12 with an indicated pH (7.4 or 9.0), or supplemented with 1 μM insulin, then lysed and blotted

with anti-pIRR/IR and anti-IRR/IR antibodies. Arrows indicate β-subunits. The Western blots shown are representative of 3 independent experiments. See also Figure S4.

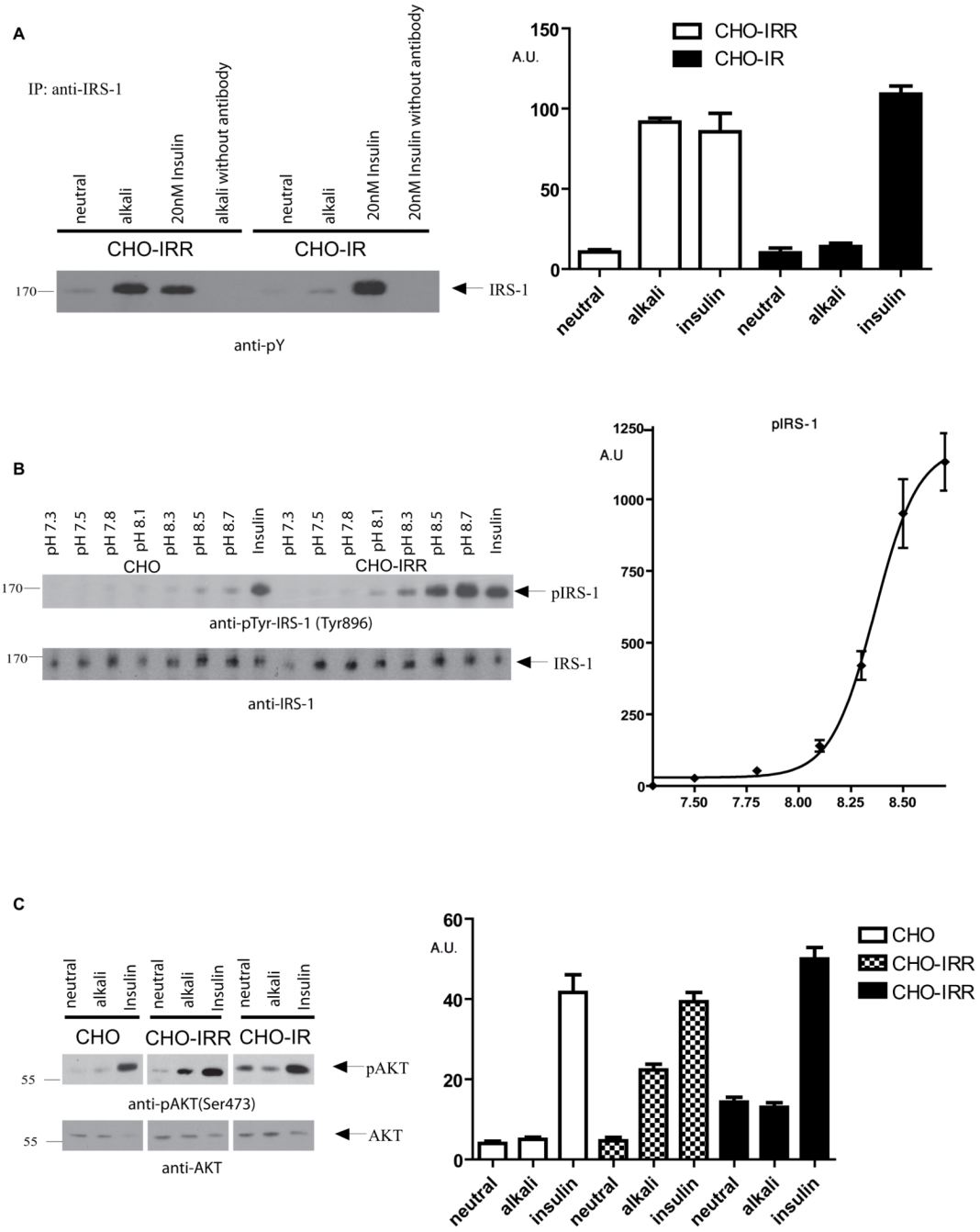

Figure 6. Intracellular cell signaling, triggered by IRR activation

(A) Phosphorylation of IRS-1 in alkali or insulin-stimulated cell lines. Non-starved IRR and IR-stably transfected cell lines were incubated for 10 min in F12 medium pH 7.4 or 9.0, then lysed and immunoprecipitated with anti-IRS-1 antibody. No antibody was added in the indicated samples as control. The precipitates were analyzed by Western blotting with anti-pY antibody. (B) pH-dependence of IRS-1 signaling. CHO and CHO-IRR cell lines were incubated for 10 min with PBS, adjusted to indicated pH with 60 mM EPPS, or with 20 nM insulin. The lysed cells were Western blotted with anti-pIRS-1 and anti-IRS-1 antibodies. (C) AKT signaling in alkali-stimulated cell lines. CHO, CHO-IRR and IR cells were treated with F-12 pH 7.4, pH 9.0, or with 1μM insulin for 10 min at 37°C. The lysed cells were

blotted with anti-pAKT, or anti-AKT antibodies. Original blots representative of 3 independent experiments are shown on left panels. Semi-quantitative densitometry data as in Figure 4 are presented on right panels. The data were normalized by total density (minus background) of each blot. Values are means ± SE. See also Figure S5.

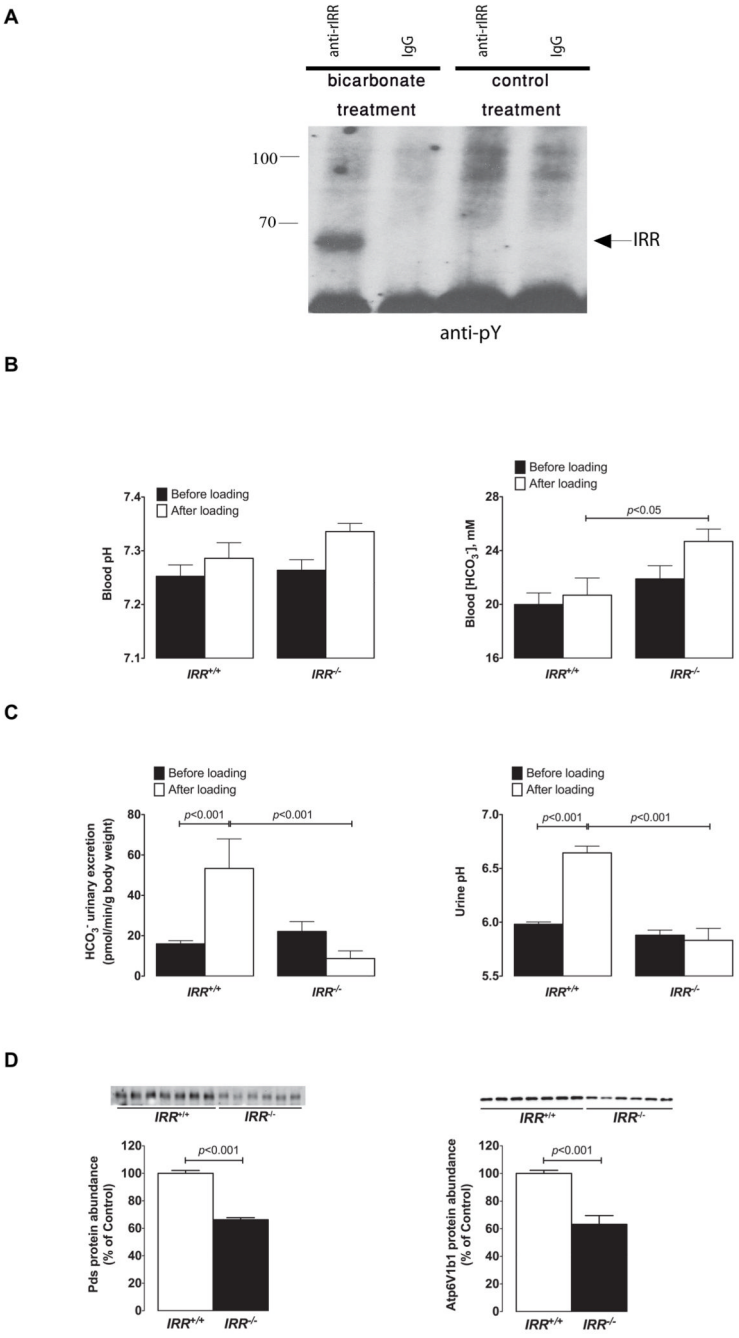

Figure 7. *In vivo* analyses of IRR function

(A) Rats were anesthetized, and their kidneys were perfused through renal arteries with 1% solution of $NaHCO_3$ or with 0.9% NaCl (control). The kidneys were then removed and immediately homogenized and extracted, as described in Experimental Procedures. The extracts were immunoprecipitated with affinity purified anti-rat IRR antibody or with the same concentration of rat IgGs as control and analyzed by Western blotting with anti-pY antibody. The blot is representative of three independent experiments. The arrow indicates position of the IRR β-subunit band. (B) Blood gas analyses in $IRR^{+/+}$ and $IRR^{-/-}$ mice before and after 7 days of alkali-load administered as 0.28M solution of $NaHCO_3$ in the drinking water. (C) Initial renal response to alkali-loading measured in $IRR^{+/+}$ and $IRR^{-/-}$

mice. Six hours urine collections (from 9h00 a.m. to 3h00 p.m.) were obtained from same $IRR^{+/+}$ and $IRR^{-/-}$ mice administrated either dionized water on the first day of the experiment (black bars) or $NaHCO_3$ solution on the second day (white bars) to measure urine pH and renal bicarbonate excretion. (D) Immunoblots of membrane fractions from the renal cortex obtained from $IRR^{+/+}$and $IRR^{-/-}$ mice after 7 days of alkali-loading. The membrane preparations were blotted with antibodies directed against Pds and Atp6v1b1. Densitometric analyses of data show the abundance of Pds, and Atp6v1b1, respectively, expressed as % of control. Equality of loading was verified by running, in parallel, gels that were stained with Coomassie blue and quantified as described previously (Quentin et al., 2004a). Values are means ± SE. See also Figure S6.